# DISPERSION AND DISSIPATION ERRORS OF TWO FULLY DISCRETE DISCONTINUOUS GALERKIN METHODS

HE YANG, FENGYAN LI, AND JIANXIAN QIU

Abstract. The dispersion and dissipation properties of numerical methods are very important in wave simulations. In this paper, such properties are analyzed for Runge-Kutta discontinuous Galerkin methods and Lax-Wendroff discontinuous Galerkin methods when solving the linear advection equation. With the standard analysis, the asymptotic formulations are derived analytically for the discrete dispersion relation in the limit of $K = kh \to 0$ ($k$ is the wavenumber and $h$ is the meshsize) as a function of the CFL number, and the results are compared quantitatively between these two fully discrete numerical methods. For Lax-Wendroff discontinuous Galerkin methods, we further introduce an alternative approach which is advantageous in dispersion analysis when the methods are of arbitrary order of accuracy. Based on the analytical formulations of the dispersion and dissipation errors, we also investigate the role of the spatial and temporal discretizations in the dispersion analysis. Numerical experiments are presented to validate some of the theoretical findings. This work provides the first analysis for Lax-Wendroff discontinuous Galerkin methods.

## 1. Introduction

In wave simulations, highly accurate numerical methods with good dispersive and dissipative behaviors are preferred. In this paper, we analyze the dispersion and dissipation errors of two fully discrete high order discontinuous Galerkin methods, namely, Runge-Kutta discontinuous Galerkin methods and Lax-Wendroff discontinuous Galerkin methods for a one-dimensional linear advection equation. Discontinuous Galerkin (DG) methods, as one class of finite element methods, use piecewise-defined approximating functions that are discontinuous at mesh interfaces. The methods can be easily designed to have arbitrary order accuracy, with the advantages of being compact, free of the inversion of any global mass matrix when solving time-dependent problems explicitly, suitable for adaptive simulation

*Key words and phrases.* Discrete dispersion relation; Runge-Kutta discontinuous Galerkin method; Lax-Wendroff discontinuous Galerkin method.

The research of F. Li and H. Yang is partially supported by NSF CAREER award DMS-0847241 and an Alfred P. Sloan Research Fellowship. The research of J. Qiu is partially supported by the National Science Foundation of China Grant No. 10931004 and ISTCP of China Grant No. 2010DFR00700.

and complicated geometry, high parallel efficiency, as well as rich mathematical theory in terms of stability and error analysis. The aforementioned properties of DG methods make them one of the most competitive methods in many applications which also include various wave equations [10, 11, 2, 4].

DG methods were originally proposed by Reed and Hill [19] to solve the linear neutron transport equation. The error analysis was established by Lesaint and Raviart [15], Johnson and Pitkäranta [14], Richter [20], and Peterson [16]. Motivated by the success for steady state problems, DG methods were further devised for many time-dependent equations. In [7], Chavent and Salzano constructed a fully discrete scheme using piecewise linear DG method as spatial discretization and the forward Euler method as time discretization, this method however relies on a very restrictive CFL condition for linear stability. Since then there have been many developments in time discretizations, in combination with DG spatial discretizations to get practically more useful schemes, among which are Runge-Kutta time discretizations and Lax-Wendroff time discretizations. The first DG method with Runge-Kutta time discretizations (RKDG) was introduced by Cockburn and Shu in [8]. The methods were generalized in [9] and are now widely used in many applications due to their simplicity and being explicit. Some error analysis was carried out for these fully discrete methods by Zhang and Shu in [24, 25, 26] and also by Zhong and Shu in [27]. DG methods with the Lax-Wendroff type time discretization (LWDG) were proposed by Qiu, Dumbser and Shu [18]. As one-step one-stage high order numerical methods, when compared with the one-step multi-stage RKDG methods, LWDG methods demonstrate cost efficiency in some applications such as two-dimensional Euler equations in gas dynamics.

There has been abundant study on the dispersion analysis of many numerical methods, with some examples including DG methods [22, 11, 12, 2, 21, 4], finite element methods [1, 13, 3], and spectral element methods [23, 5, 6]. Most work was carried out for semi-discrete schemes. In particular, among the dispersion analysis for DG methods, Sherwin [22] studied the dispersion relation of the semi-discrete continuous and discontinuous Galerkin methods for the linear advection equation. He obtained analytically the dispersion relation when the discrete spaces involve polynomials of degree up to 3, in addition to a numerical study when the polynomial degree is up to 10. Hu and Atkins [11] examined the semi-discrete DG methods for one- and two-dimensional linear advection equation with the limit $kh \to 0$ ($k$ is wavenumber, $h$ is the meshsize). They derived the analytical formulations of dispersion and dissipation errors when the polynomials degree is up to 16, and conjectured the formulations for general cases in terms of some Padé approximants. This conjecture was proved in [2] by Ainsworth, where he also considered the dispersion relation of $hp$ DG methods in two other limits. Later, Ainsworth, Monk and Muniz [4] studied the dispersive and dissipative behavior of semi-discrete DG methods for the acoustic wave

equation based on either the interior penalty DG methods for the second order wave equation or a general DG method applied to the wave equation in its first order form. In terms of fully discrete DG methods, there is much less work on the dispersion analysis. Sármány et al. in [21] considered the DG methods with Runge-Kutta time discretization for Maxwell equations. They numerically evaluated the accuracy order of the dispersion and dissipation errors of the methods.

In the present work, we focus on the *fully discrete* DG methods and derive *analytical* formulations of the dispersion and dissipation errors of both RKDG and LWDG methods in terms of the CFL number for $kh \ll 1$, with which we carry out comparison between these two methods and further gain insightful understanding towards the roles of the temporal and spatial discretizations in dispersion and dissipation behavior. In particular, it is shown that the DG spatial discretizations lead to super-convergence in the dispersion and dissipation errors compared with the accuracy of the methods in the $L^2$ norm. This is consistent to the results for the semi-discrete DG methods [11, 2]. However, when Runge-Kutta methods with matching accuracy or the Lax-Wendroff type methods are used as the time discretizations, such super-convergence property is largely lost with the CFL number being order one. We believe this is due to the finite difference nature of the time discretizations. The work in this paper also provides the first (dispersion) analysis for LWDG methods, which have comparable asymptotic dispersion and dissipative behavior as RKDG methods of the same order. For this class of one-step methods, an alternative dispersion analysis is further performed, and it proves to be advantageous for the methods with arbitrary order of accuracy.

The remaining of this paper is organized as follows. In section 2, RKDG and LWDG methods are introduced for general one-dimensional conservation laws. In section 3, we first follow the standard dispersion analysis to obtain the analytical discrete dispersion relation of these two methods when solving the linear advection equation. Such relations are given asymptotically in $kh \ll 1$ as a function of the CFL number. With these results, comparison is carried out between RKDG and LWDG methods in their dispersion and dissipation behavior. In section 3, an alternative dispersion analysis is also given for LWDG methods which can be used to easily analyze the methods when they are of any order of accuracy. By examining the dispersion and dissipation errors when the CFL number is sufficiently small, in section 4, we further gain insight for the roles of the spatial and temporal discretizations in the dispersion analysis. In section 5, numerical experiments are presented to validate some of our theoretical findings, which are followed by concluding remarks in section 6.

## 2. Formulations of discontinuous Galerkin methods

In this section, we will introduce Runge-Kutta discontinuous Galerkin methods and Lax-Wendroff discontinuous Galerkin methods for a one-dimensional scalar conservation law

$$u_t + f(u)_x = 0,\ x \in [a,b],\ t > 0. \tag{2.1}$$

These are two fully discrete methods which can be of any order of accuracy. Let $a = x_{\frac{1}{2}} < x_{\frac{3}{2}} < \cdots < x_{m+\frac{1}{2}} = b$ be a partition of the computational domain, with each element denoted as $I_j = [x_{j-\frac{1}{2}}, x_{j+\frac{1}{2}}]$, the midpoint of $I_j$ as $x_j = (x_{j-\frac{1}{2}} + x_{j+\frac{1}{2}})/2$, and the length as $h_j$. We define the approximation space as

$$V_h^N = \{v : v|_{I_j} \in P^N(I_j), j = 1, \ldots, m\},$$

where $P^N(I_j)$ is the space of polynomials of degree at most $N$ on $I_j$. All functions in $V_h^N$ are piecewise polynomials, and they are discontinuous at gridpoints. For any $v \in V_h^N$, we also denote $v^-_{j+\frac{1}{2}} = \lim_{\epsilon\to 0-} v(x_{j+\frac{1}{2}} + \epsilon)$ and $v^+_{j-\frac{1}{2}} = \lim_{\epsilon\to 0+} v(x_{j-\frac{1}{2}} + \epsilon)$, $\forall j$.

The semi-discrete discontinuous Galerkin method for (2.1) is to look for an approximated solution $u_h \in V_h^N$ such that for any $v \in V_h^N$ and $j = 1, \ldots, m$, there is

$$\int_{I_j} (u_h)_t v dx - \int_{I_j} f(u_h) v_x dx + \hat{f}_{j+\frac{1}{2}} v^-_{j+\frac{1}{2}} - \hat{f}_{j-\frac{1}{2}} v^+_{j-\frac{1}{2}} = 0. \tag{2.2}$$

Here $\hat{f}_{j+\frac{1}{2}}(u_h)$ is a numerical flux at $x_{j+\frac{1}{2}}$ that depends on $u^-_{h,j+\frac{1}{2}}$ and $u^+_{h,j+\frac{1}{2}}$, $\forall j$. If we take $\{v_l^j(x), l = 0, 1, \ldots, N\}$ as a local basis of $V_h^N$ on $I_j$ and represent the numerical solution as $u_h(x,t)|_{I_j} = \sum_{l=0}^N C_l^j(t) v_l^j(x)$, then equation (2.2) with $j = 1, \ldots, m$ will become an ODE system for $\{C_l^j(t)\}_{j,l}$. If we further solve this ODE system by Runge-Kutta time discretizations, this will give Runge-Kutta discontinuous Galerkin (RKDG) methods for equation (2.1). In section 3, an equivalent formulation of (2.2), namely,

$$\int_{I_j} (u_h)_t v dx + \int_{I_j} f(u_h)_x v dx = (f^-_{j+\frac{1}{2}} - \hat{f}_{j+\frac{1}{2}}) v^-_{j+\frac{1}{2}} - (f^+_{j-\frac{1}{2}} - \hat{f}_{j-\frac{1}{2}}) v^+_{j-\frac{1}{2}} \tag{2.3}$$

will be used to derive the discrete dispersion relation.

The Lax-Wendroff discontinuous Galerkin (LWDG) method starts with a Taylor expansion of the solution $u$ in time,

$$u(x, t+\Delta t) = u(x,t) + \Delta t u_t + \frac{\Delta t^2}{2} u_{tt} + \frac{\Delta t^3}{6} u_{ttt} + \ldots. \tag{2.4}$$

Here we use $\Delta t$ to denote the time step. In order to obtain $(N+1)^{st}$ order temporal accuracy, we will keep the first $N+1$ time derivatives in (2.4) and replace them with spatial derivatives based on the original partial differential

equation (2.1). For instance, for third order accuracy in time with $N = 2$, we will replace $u_t, u_{tt}$ and $u_{ttt}$ in (2.4) with

$$u_t = -f(u)_x, \;\; u_{tt} = \left((f')^2 u_x\right)_x, \;\; u_{ttt} = -\left(3(f')^2(f'')(u_x)^2 + (f')^3 u_{xx}\right)_x,$$

and approximate $u(x, t + \Delta t)$ by

$$u(x, t + \Delta t) \approx u(x, t) - \Delta t F_x,$$

where

$$F = f(u) - \frac{\Delta t}{2}(f')^2 u_x + \frac{\Delta t^2}{6}\left(3(f')^2(f'')(u_x)^2 + (f')^3 u_{xx}\right). \tag{2.5}$$

Note that function $F$ should be $F_N$, and we will drop the subscript $N$ for the simplicity of notations.

With $V_h^N$ as the approximation space, the LWDG method is given as follows: look for the solution $u_h \in V_h^N$ satisfying

$$\int_{I_j} u_h(x, t+\Delta t) v dx = \int_{I_j} u_h(x,t) v dx + \Delta t \int_{I_j} F(u_h) v_x dx - \Delta t(\hat{F}_{j+\frac{1}{2}} v^-_{j+\frac{1}{2}} - \hat{F}_{j-\frac{1}{2}} v^+_{j-\frac{1}{2}}), \tag{2.6}$$

for any $v \in V_h^N$ and $j = 1, \ldots, m$. Here $\hat{F}$ is a numerical flux, which will be defined in section 3.2 for a specific $f(u)$ considered in this paper. The resulting method is formally $(N+1)^{st}$ order accurate in both space and time, and it will be termed as LWDG(N+1).

With the same notation of the local basis and the solution representation as for the RKDG method, the LWDG method can be further converted into an algebraic system for $\{C_l^j(t_n)\}_{j,l,n}$,

$$\sum_{l=0}^{N} \int_{I_j} v_l^j v_i^j dx \left(C_l^j(t_{n+1}) - C_l^j(t_n)\right) = \Delta t \int_{I_j} (v_i^j)_x F dx - \Delta t \left(\hat{F}_{j+\frac{1}{2}}(v_i^j)^-_{j+\frac{1}{2}} - \hat{F}_{j-\frac{1}{2}}(v_i^j)^+_{j-\frac{1}{2}}\right), \tag{2.7}$$

for $i = 0, 1, \ldots, N$ and $j = 1, \ldots, m$. Here $\{t_n\}_n$ is for the discrete time, and $t_{n+1} = t_n + \Delta t$. The timestep $\Delta t$ can depend on $n$ in practice. A mathematically equivalent form of (2.7) is given as follows,

$$\begin{aligned} \sum_{l=0}^{N} \int_{I_j} v_l^j v_i^j dx \left(C_l^j(t_{n+1}) - C_l^j(t_n)\right) =& -\Delta t \int_{I_j} F_x v_i^j dx \\ &+ \Delta t \left((F^-_{j+\frac{1}{2}} - \hat{F}_{j+\frac{1}{2}})(v_i^j)^-_{j+\frac{1}{2}} - (F^+_{j-\frac{1}{2}} - \hat{F}_{j-\frac{1}{2}})(v_i^j)^+_{j-\frac{1}{2}}\right), \end{aligned} \tag{2.8}$$

and it will be used in next section in the dispersion analysis.

## 3. Dispersion analysis

In this paper, we focus on the dissipation and dispersion analysis for the fully discrete RKDG methods and LWDG methods defined in section 2 when they are applied to the linear advection equation

$$u_t + u_x = 0, \; x \in (0, 2\pi], \; t > 0. \tag{3.1}$$

with periodic boundary condition. This corresponds to equation (2.1) with $f(u) = u$, $a = 0$, and $b = 2\pi$. Without loss of generality, the mesh is assumed to be uniform with $h_j = h$ for any $j$. We choose an orthogonal local basis, given by the scaled translated Legendre polynomials $v_l^j(x) = \sqrt{\frac{2l+1}{2}} P_l\left(\frac{2(x-x_j)}{h}\right)$. Here $P_l(x)$ with $l = 0, \ldots, N$ are the Legendre polynomials on $[-1, 1]$ satisfying $P_l(1) = 1$. We also define the coefficient vector $\boldsymbol{C^j} = (C_0^j, C_1^j, \ldots, C_N^j)^T$, where $C_l^j$ with $l = 0, 1, \ldots, N$ are the coefficients in the local expansion of $u_h$.

In order to carry out the dispersion analysis, we consider the linear advection equation (3.1) with an initial condition $u(x, 0) = e^{ikx}$. The exact solution is given by $u(x, t) = e^{i(kx-\omega t)}$ with $\omega = k$. Here $k$ is called the wavenumber, $\omega$ is the frequency, and $\omega = k$ is the exact dispersion relation for equation (3.1). Suppose the numerical solution of a method is of the same form, namely, $u_h(x, t) = e^{i(kx-\tilde{\omega}t)} = e^{\omega_i t} e^{i(kx-\omega_r t)}$. When $\omega_i = \Im(\tilde{\omega}) < 0$, the scheme is dissipative. And $\omega_r = \Re(\tilde{\omega}) \neq k$ gives a dispersive solution. By taking into account how fine the mesh is with respect to the wavenumber $k$, we further define $K = kh$ and $\Omega = \Omega_r + i\Omega_i$ with $\Omega_r = \omega_r h$ and $\Omega_i = \omega_i h$, then the exact dispersion relation can be expressed as $\Omega_r = K$ and $\Omega_i = 0$. Our goal is to estimate the dispersion error $\Omega_r - K$ and the dissipation error $\Omega_i$ of the RKDG and LWDG methods with respect to the CFL number $\nu = \frac{\Delta t}{h}$ for $K \ll 1$. In this paper, all reference values of the CFL number to ensure the linear stability of the scheme come from literature.

3.1. **Analysis of RKDG methods.** To allow information propagate stably, we use an upwind numerical flux for the semi-discrete DG method in (2.3) when it is applied to (3.1). That is, $\hat{f}_{j+\frac{1}{2}} = \hat{u}_{h,j+\frac{1}{2}} = u^-_{h,j+\frac{1}{2}}$, $\forall j$. Then the method becomes

$$\begin{aligned} \int_{I_j} u_{h,t} v dx + \int_{I_j} u_{h,x} v dx &= (u^-_{h,j+\frac{1}{2}} - \hat{u}_{h,j+\frac{1}{2}}) v^-_{j+\frac{1}{2}} - (u^+_{h,j-\frac{1}{2}} - \hat{u}_{h,j-\frac{1}{2}}) v^+_{j-\frac{1}{2}} \\ &= -(u^+_{h,j-\frac{1}{2}} - u^-_{h,j-\frac{1}{2}}) v^+_{j-\frac{1}{2}} \end{aligned} \tag{3.2}$$

for $j = 1, \ldots, m$, and it can be further written into a matrix form

$$\frac{d\boldsymbol{C}^j}{dt} = \frac{2}{h}\left(-(D_0 + G_0^+)\boldsymbol{C}^j + G_0^- \boldsymbol{C}^{j-1}\right), \tag{3.3}$$

once the solution representation is taken in terms of the local basis. Here the $(s, l)$-th entry of the matrices $D_0, G_0^-, G_0^+$ is defined as

$$D_0(s, l) = \int_{I_j} v_s^j \frac{\partial v_l^j}{\partial x} dx, G_0^-(s, l) = (v_s^j v_l^{j-1})|_{x_{j-\frac{1}{2}}}, G_0^+(s, l) = (v_s^j v_l^j)|_{x_{j-\frac{1}{2}}},$$

respectively. It is easy to see that these matrices are independent of index $j$, therefore the notations $D_0, G_0^+$ and $G_0^-$ will not lead to any confusion.

With $U = -(D_0 + G_0^+), L = G_0^-$, we rewrite equation (3.3) with $j = 1, \ldots, m$ into an ODE system

$$\begin{pmatrix} \frac{d\boldsymbol{C}^1}{dt} \\ \frac{d\boldsymbol{C}^2}{dt} \\ \vdots \\ \vdots \\ \frac{d\boldsymbol{C}^m}{dt} \end{pmatrix} = \frac{2}{h} \begin{pmatrix} U & 0 & \ldots & 0 & L \\ L & U & & & \\ & \ddots & \ddots & & \\ & & \ddots & \ddots & \\ & & & L & U \end{pmatrix} \begin{pmatrix} \boldsymbol{C}^1 \\ \boldsymbol{C}^2 \\ \vdots \\ \vdots \\ \boldsymbol{C}^m \end{pmatrix} \tag{3.4}$$

which can also be compactly denoted as $\frac{d\boldsymbol{C}}{dt} = A\boldsymbol{C}$, with $A$ being the coefficient matrix and $\boldsymbol{C} = ((\boldsymbol{C}^1)^T, \ldots, (\boldsymbol{C}^m)^T)^T$. We then solve this ODE system from time $t$ to $t+\Delta t$ by Runge-Kutta (RK) methods. For instance, the 2-stage $2^{nd}$ order RK method gives $\boldsymbol{C}(t+\Delta t) = \left(I + \Delta t A + \frac{1}{2}(\Delta t A)^2\right)\boldsymbol{C}(t)$, and the 3-stage $3^{rd}$ order RK method gives $\boldsymbol{C}(t+\Delta t) = \left(I + \Delta t A + \frac{1}{2}(\Delta t A)^2 + \frac{1}{6}(\Delta t A)^3\right)\boldsymbol{C}(t)$. In this paper, we will use RKDG(N+1) to denote the fully discrete scheme which uses the upwind DG method in (3.4) (also see (3.2)) with the discrete space $V_h^N$ as the spatial discretization, and the $(N+1)$-stage $(N+1)^{st}$ order RK method as the time discretization.

3.1.1. *RKDG2 with $N = 1$.* With a simple derivation, RKDG2 can be written as

$$\begin{aligned} \boldsymbol{C}^j(t+\Delta t) = {} & 2\nu^2 L^2 \boldsymbol{C}^{j-2}(t) + \left(2\nu L + 2\nu^2(LU+UL)\right)\boldsymbol{C}^{j-1}(t) \\ & + \left(I + 2\nu U + 2\nu^2 U^2\right)\boldsymbol{C}^j(t). \end{aligned} \tag{3.5}$$

Let $\boldsymbol{C}^j(t) = \boldsymbol{\alpha}\exp(i(kx_j - \tilde{\omega}t))$, with $\boldsymbol{\alpha}$ being a nonzero constant vector of length $N+1$. We substitute it into equation (3.5) and obtain an eigenvalue problem

$$(e^{-i\tilde{\omega}\Delta t} I - \mathcal{M})\boldsymbol{\alpha} = 0, \tag{3.6}$$

where

$$\mathcal{M} = 2\nu^2 L^2 e^{-2ikh} + \left(2\nu L + 2\nu^2(LU+UL)\right)e^{-ikh} + I + 2\nu U + 2\nu^2 U^2. \tag{3.7}$$

This $2\times 2$ matrix $\mathcal{M}$ has two eigenvalues, and if we denote one as $\lambda$, then

$$\begin{cases} \Omega_r = -\frac{1}{\nu}\arctan\left(\frac{\Im(\lambda)}{\Re(\lambda)}\right), \\ \Omega_i = \frac{1}{2\nu}\ln\left((\Re(\lambda))^2 + (\Im(\lambda))^2\right). \end{cases} \tag{3.8}$$

For $K = kh \ll 1$, there is only one eigenvalue of $\mathcal{M}$, satisfying $\Omega_r \sim K$ as $K \to 0$, which is physically relevant and is said to be consistent. Based on the consistent eigenvalue of $\mathcal{M}$ in (3.7), we obtain

$$\begin{cases} \Omega_r = K + \frac{1}{6}\nu^2 K^3 + \left(\frac{1}{270} - \frac{1}{20}\nu^4\right)K^5 + O(K^7), \\ \Omega_i = \left(-\frac{1}{72} + \frac{1}{8}\nu^3\right)K^4 + \left(\frac{1}{648} - \frac{1}{144}\nu^2\right)K^6 + O(K^8). \end{cases} \tag{3.9}$$

This indicates that the dispersion error $\Omega_r - K$ is of third order accuracy with respect to $K \ll 1$, and the dissipation error $\Omega_i$ is of fourth order accuracy. When $k = O(1)$, this is equivalent to say that the dispersion error $\omega_r - k$

is of second order accuracy and the dissipation error $\omega_i$ is of third order accuracy in $h \ll 1$.

It seems that a careful selection of the CFL number $\nu$ may lead to $-\frac{1}{72} + \frac{1}{8}\nu^3 = 0$ and therefore give higher accuracy in dissipation error. However, to make this happen, one must choose $\nu \approx 0.4807$, which is beyond the linear stability limit of RKDG2, $\nu \leq \frac{1}{3}$. In other words, the result in (3.9) is sharp, and no higher order accuracy can be achieved for either the dissipative error or the dispersive error by simply changing the constant $\nu$. (Later in section 4, a different scenario is discussed when $\nu$ is allowed to depend on $K$.) Note that the dominating error is from dispersion, and the coefficient of its leading term is an increasing function of $\nu$ and it is always positive. Therefore a smaller CFL number leads to a smaller dispersion error. On the other hand, since $|-\frac{1}{72} + \frac{1}{8}\nu^3|$ increases as $\nu \to 0+$, a smaller CFL number leads to a larger dissipation error.

For a given wavenumber $k$, by making use of the asymptotic formula in (3.9), we can estimate the total dispersion and dissipation errors of the RKDG2 solution up to a given time $T$ for sufficiently small mesh size $h$. To be more concrete, assume the numerical solution is

(3.10)
$$u_h(x,T) = e^{i(kx-\tilde{\omega}T)} = e^{\Im(\tilde{\omega})T} e^{i(kx-\Re(\tilde{\omega})T)} = e^{\Omega_i \frac{T}{h}} e^{i(K-\Omega_r)\frac{T}{h}} e^{i(kx-kT)},$$

then $e^{\Omega_i \frac{T}{h}} \sim e^{\left(-\frac{1}{72}+\frac{1}{8}\nu^3\right)K^4\frac{T}{h}}$ measures the total dissipation error, and $e^{i(K-\Omega_r)\frac{T}{h}} \sim e^{-\frac{1}{6}i\nu^2K^3\frac{T}{h}}$ measures the total dispersion error up to time $T$. These approximations can provide useful guidance for one to control errors in wave simulations.

3.1.2. *RKDG3 with $N = 2$.* Following the similar procedure for RKDG2, we obtain an eigenvalue problem (3.6) for the dispersion analysis of RKDG3, where $\mathcal{M} = A_1 e^{-3ikh} + A_2 e^{-2ikh} + A_3 e^{-ikh} + A_4$ with

$$\begin{aligned}
A_1 &= \frac{4}{3}\nu^3 L^3, \\
A_2 &= \frac{4}{3}\nu^3(L^2U + LUL + UL^2) + 2\nu^2 L^2, \\
A_3 &= \frac{4}{3}\nu^3(LU^2 + ULU + U^2L) + 2\nu^2(LU + UL) + 2\nu L, \\
A_4 &= I + \frac{4}{3}\nu^3 U^3 + 2\nu^2 U^2 + 2\nu U.
\end{aligned}$$

When we use symbolic computation software **MAPLE** to obtain the consistent eigenvalues of $\mathcal{M}$, in order to simplify the lengthy result and get an analytical form of the leading term, the following nontrivial equality is identified and proves to be crucial,

$$\begin{aligned}
&52 + 72\nu - 3240\nu^2 + 8260\nu^3 + 6360\nu^4 - 11568\nu^5 - 33408 \\
&\quad + \sqrt{17}(20 - 120\nu + 120\nu^2 - 420\nu^3 + 3720\nu^4 - 3600\nu^5 - 8000\nu^6)
\end{aligned}$$

$$= (1 + 7\nu - 24\nu^2 + \sqrt{17} - 3\sqrt{17}\nu - 4\sqrt{17}\nu^2)^3.$$

With this, the consistent eigenvalue of $\mathcal{M}$ is simply given by

$$\lambda = 1 - i\nu K - \frac{1}{2}\nu^2 K^2 + i\frac{1}{6}\nu^3 K^3 + O(K^6),$$

and we further obtain from (3.8)

$$\begin{cases} \Omega_r = K + \frac{1}{30}\nu^4 K^5 + (\frac{1}{42000} - \frac{1}{252}\nu^6)K^7 + O(K^8), \\ \Omega_i = -\frac{1}{24}\nu^3 K^4 + (\frac{1}{72}\nu^5 - \frac{1}{7200})K^6 + O(K^8). \end{cases} \tag{3.11}$$

One can see that the dissipation error of RKDG3 is of the same order of accuracy as that of RKDG2, and Figure 3.1 (left) further shows that RKDG3 has smaller dissipation error regardless of the CFL number $\nu$. We only plot the curve with $\nu \in [0, 0.2]$ for RKDG3 due to its linear stability condition $\nu < 0.209$. On the other hand, the dispersion error of RKDG3 is fifth order accurate, and it is much higher compared with RKDG2. Moreover, for RKDG3, the dissipation error is dominating, and a smaller CFL number leads to smaller dissipation and dispersion errors and thus more accurate solutions.

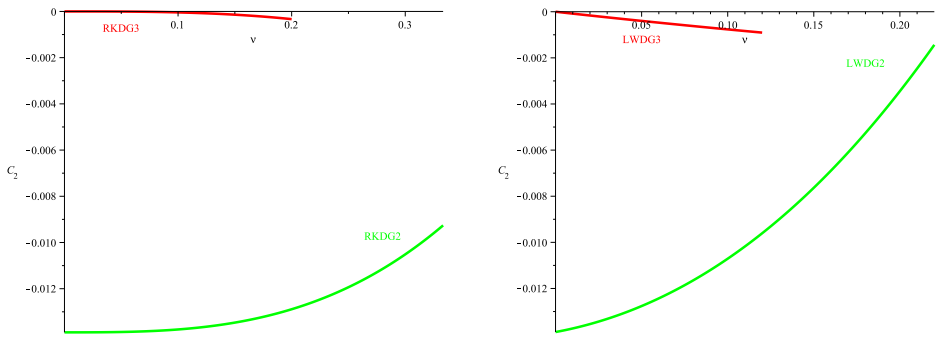


FIGURE 3.1. The leading coefficient $C_2$ in the dissipation error $\Omega_i = C_2 K^4 + O(K^6)$. Left: RKDG2 and RKDG3; Right: LWDG2 and LWDG3.

3.2. **Analysis of LWDG methods.** For the linear advection equation (3.1) with $f(u) = u$, the function $F$ in (2.5) with general $N$ becomes

$$F = u - \frac{\Delta t}{2!}u_x + \frac{(\Delta t)^2}{3!}u_{xx} + \ldots + (-1)^N \frac{(\Delta t)^N}{(N+1)!}\frac{\partial^N u}{\partial x^N}.$$

Consider the following numerical flux for the LWDG method in (2.7) (or in (2.8)),

$$\hat{F}_{j+\frac{1}{2}} = \beta u^-_{j+\frac{1}{2}} + (1-\beta)u^+_{j+\frac{1}{2}} + \gamma(F-u)^-_{j+\frac{1}{2}} + (1-\gamma)(F-u)^+_{j+\frac{1}{2}} \tag{3.12}$$

with parameters $\beta, \gamma \in [0, 1]$. Different values of $\beta$ and $\gamma$ will give different numerical fluxes, and one shall know that not all values lead to stable schemes. One widely-used numerical flux for the LWDG method is with

$\beta = 1, \gamma = \frac{1}{2}$. In this subsection, we will focus on the dispersion analysis of the LWDG method with this numerical flux.

In order to derive the compact matrix form of the LWDG method, we define matrices $E^-, E^+, G^-, G^+$ and $D$, which all depend on $N$ and have the $(s,l)$-th entries given as follows.

(3.13)

$$E^-(s,l) = \left( (1-\beta) v_s^j v_l^j + (1-\gamma)(-\frac{\Delta t}{2!} v_s^j \frac{\partial v_l^j}{\partial x} + \ldots + (-1)^N \frac{(\Delta t)^N}{(N+1)!} v_s^j \frac{\partial^N v_l^j}{\partial x^N}) \right)_{x_{j+\frac{1}{2}}},$$

$$E^+(s,l) = \left( (1-\beta) v_s^j v_l^{j+1} + (1-\gamma)(-\frac{\Delta t}{2!} v_s^j \frac{\partial v_l^{j+1}}{\partial x} + \ldots + (-1)^N \frac{(\Delta t)^N}{(N+1)!} v_s^j \frac{\partial^N v_l^{j+1}}{\partial x^N}) \right)_{x_{j+\frac{1}{2}}},$$

$$G^-(s,l) = \left( \beta v_s^j v_l^{j-1} + \gamma(-\frac{\Delta t}{2!} v_s^j \frac{\partial v_l^{j-1}}{\partial x} + \ldots + (-1)^N \frac{(\Delta t)^N}{(N+1)!} v_s^j \frac{\partial^N v_l^{j-1}}{\partial x^N}) \right)_{x_{j-\frac{1}{2}}},$$

$$G^+(s,l) = \left( \beta v_s^j v_l^j + \gamma(-\frac{\Delta t}{2!} v_s^j \frac{\partial v_l^j}{\partial x} + \ldots + (-1)^N \frac{(\Delta t)^N}{(N+1)!} v_s^j \frac{\partial^N v_l^j}{\partial x^N}) \right)_{x_{j-\frac{1}{2}}},$$

$$D(s,l) = \int_{I_j} v_s^j \frac{\partial v_l^j}{\partial x} dx - \frac{\Delta t}{2!} \int_{I_j} v_s^j \frac{\partial^2 v_l^j}{\partial x^2} dx + \ldots + (-1)^N \frac{(\Delta t)^{N-1}}{N!} \int_{I_j} v_s^j \frac{\partial^N v_l^j}{\partial x^N} dx.$$

Using these matrices, the LWDG method in (2.8) can be rewritten as

(3.14)

$$\frac{1}{2\nu} \left( \boldsymbol{C^j}(t+\Delta t) - \boldsymbol{C^j}(t) \right) = (E^- - G^+ - D)\boldsymbol{C^j}(t) + G^- \boldsymbol{C^{j-1}}(t) - E^+ \boldsymbol{C^{j+1}}(t).$$

To carry out the dispersion analysis, we take the ansatz $\boldsymbol{C}^j(t) = \boldsymbol{\alpha} \exp(i(kx_j - \tilde{\omega} t))$ in (3.14), with $\boldsymbol{\alpha}$ being a nonzero constant vector, and obtain the following eigenvalue problem

$$\left( \frac{e^{-i\tilde{\omega}\Delta t} - 1}{2\nu} I + \mathcal{M} \right) \boldsymbol{\alpha} = \mathbf{0}, \tag{3.15}$$

where $M = (D + G^+ - E^-) + E^+ e^{ikh} - G^- e^{-ikh}$. If one of the eigenvalues of $\mathcal{M}$ is denoted as $\lambda$ and let $\tilde{\lambda} = 1 - 2\nu\lambda$, we will have

$$\begin{cases} \Omega_r = \Re(\tilde{\omega})h = -\frac{1}{\nu} \arctan\left( \frac{\Im(\tilde{\lambda})}{\Re(\tilde{\lambda})} \right), \\ \Omega_i = \Im(\tilde{\omega})h = \frac{1}{2\nu} \ln\left( (\Re(\tilde{\lambda}))^2 + (\Im(\tilde{\lambda}))^2 \right). \end{cases} \tag{3.16}$$

3.2.1. *LWDG2 with $N = 1$.* For LWDG2, the physically relevant dispersion relation is given as

$$\begin{cases} \Omega_r = K + \left( \frac{1}{12}\nu + \frac{1}{6}\nu^2 \right) K^3 + O(K^5), \\ \Omega_i = \left( -\frac{1}{72} + \frac{1}{72}\nu + \frac{1}{6}\nu^2 + \frac{1}{8}\nu^3 \right) K^4 + O(K^6). \end{cases}$$

This indicates that the dispersion error $\Omega_r - K$ is dominating, and it is of third order accuracy with respect to $K \ll 1$. The dissipation error $\Omega_i$ is of fourth order accuracy. Based on [17], the linear stability condition of LWDG2 is $\nu < \nu_0 = 0.223$. Under this constraint, it can be shown that $-\frac{1}{72} + \frac{1}{72}\nu + \frac{1}{6}\nu^2 + \frac{1}{8}\nu^3 < 0$, and therefore the dissipation error of LWDG2 can not be higher than fourth order accurate. Furthermore, the leading coefficients of both $\Omega_r - K$ and $\Omega_i$ are increasing functions of $\nu$, hence a smaller CFL number $\nu$ will lead to better dispersion behavior but worse dissipation behavior of the scheme.

3.2.2. *LWDG3 with $N = 2$.* By using the following nontrivial equality

$$\begin{aligned}&\left(-52 - 360\nu - 300\nu^2 + 1000\nu^3 + 20(1+3\nu)\sqrt{17 + 30\nu - 75\nu^2}\right)^{\frac{1}{3}} \\ &= -(5\nu + 1) + \sqrt{17 + 30\nu - 75\nu^2},\end{aligned}$$

we obtain the consistent eigenvalue of $\mathcal{M}$,

$$\begin{aligned}\lambda = \frac{1}{2}iK + \frac{1}{4}\nu K^2 - \frac{1}{12}i\nu^2 K^3 - \frac{1}{240}\frac{(20\nu^3 + 5\nu^2 - 2\nu - 1)\nu}{1+3\nu}K^4 \\ + \frac{1}{3600}\frac{(300\nu^5 + 150\nu^4 - 5\nu^3 - 75\nu^2 - 7\nu + 9)\nu}{(1+3\nu)^2}iK^5 + O(K^6),\end{aligned}$$

which gives

$$\begin{cases} \Omega_r = K - \frac{1}{1800}\frac{(60\nu^5 + 15\nu^4 - 70\nu^3 - 8\nu - 9)\nu}{(1+3\nu)^2}K^5 + O(K^7), \\ \Omega_i = \frac{1}{120}\frac{(5\nu^3 - 2\nu - 1)\nu}{1+3\nu}K^4 + O(K^6). \end{cases}$$

This shows that the dissipation error dominates and it is fourth order accurate. This error is of the same order as that of LWDG2, yet the leading coefficient is of smaller magnitude, see Figure 3.1 (right). The dispersion error of LWDG3, on the other hand, is of fifth order which is two order higher than that of LWDG2. Based on [17], the linear stability condition for LWDG3 is $\nu < 0.127$. Under this restriction, Figure 3.1 (right) and Figure 3.3 (left) imply that the leading coefficient of $\Omega_r - K$ is positive and monotonically increasing, while the leading coefficient of $\Omega_i$ is negative and monotonically decreasing. In other words, as the CFL number $\nu$ decreases, the magnitude of both coefficients decreases correspondingly. Therefore, different from LWDG2, a smaller $\nu$ gives smaller dispersion and dissipation errors and therefore better accuracy in solutions.

3.3. **Comparison of RKDG and LWDG methods.** In this subsection, we compare the performance of RKDG and LWDG methods based on the formulas derived in section 3.1-3.2 for $\Omega_r$ and $\Omega_i$. Since $\Omega_r - K = C_1 K^3 + O(K^5)$ and $\Omega_i = C_2 K^4 + O(K^6)$ for both RKDG2 and LWDG2, one only needs to compare $C_l$, $l = 1, 2$ directly.

In Figure 3.2 (left), we plot the coefficient $C_1$ as a function of the CFL number $\nu$ for both RKDG2 and LWDG2. Even though the range of $\nu$ is

taken as $(0, \frac{1}{3})$, the curve for LWDG2 is valid only for $\nu \in (0, 0.223)$ due to the linear stability restriction. Both curves are monotonically increasing, and for the same $\nu$, RKDG2 has smaller dispersion error than LWDG2. In addition, with a widely used CFL number, namely, $\frac{1}{3}$ for RKDG2 and 0.22 for LWDG2, we have $C_1 = 1.85E\text{-}2$ for RKDG2 and $C_1 = 2.33E\text{-}2$ for LWDG2. Therefore, even in this case, RKDG2 still has better performance in dispersion behavior. Figure 3.2 (right) gives the curves of the coefficient $C_2$ of RKDG2 and LWDG2, and both are increasing functions of $\nu$. Within the stability range of LWDG2, both functions are negative. For a fixed $\nu$ in this range, LWDG2 has better dissipation behavior than RKDG2. This is also true if $\nu = \frac{1}{3}$ is taken for RKDG2 and $\nu = 0.22$ is for LWDG2.

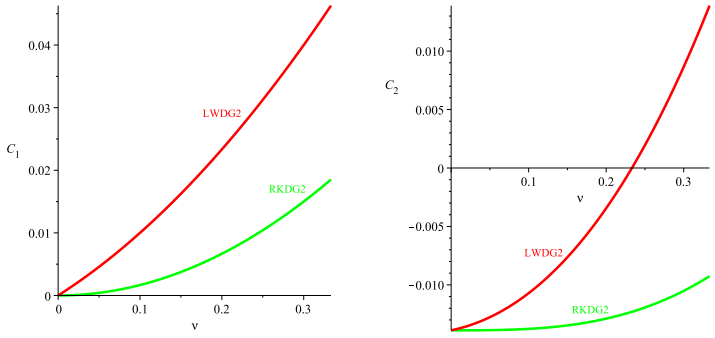


FIGURE 3.2. Left: The leading coefficient $C_1$ in the dispersion error $\Omega_r = K + C_1K^3 + O(K^5)$ for RKDG2 and LWDG2. Right: The leading coefficient $C_2$ in the dissipation error $\Omega_i = C_2K^4 + O(K^6)$ for RKDG2 and LWDG2.

For RKDG3 and LWDG3 with $N = 2$, there are $\Omega_r - K = C_1K^5 + O(K^7)$ and $\Omega_i = C_2K^4 + O(K^6)$. Figure 3.3 shows that both $C_1$ and $C_2$ for RKDG3 are of much smaller magnitude than those for LWDG3, therefore RKDG3 has better dispersion and dissipation behavior with more accurate numerical solutions than LWDG3. Note that for $N = 1, 2$, both RKDG and LWDG methods have positive $C_1$. This implies a phase lead, which is confirmed by numerical experiments in section 5 (see Table 5.1 and Table 5.3).

When $N \geq 3$, for the eigenvalue problems arising in the dispersion analysis of RKDG(N+1) and LWDG(N+1), we can no longer obtain a compact asymptotic formula of the consistent eigenvalue as a function of the CFL number $\nu$ with respect to $K \ll 1$, hence we will not include any discussion for these cases. One can surely numerically evaluate the dispersion relation with a given $\nu$ for larger $N$ as in [21] by following the analysis in sections 3.1 and 3.2.

3.4. **An alternative analysis for LWDG methods: the fixed-$\omega$ method.** The dispersion analysis in sections 3.1-3.2 is a standard approach, which solves the eigenvalue problem (3.6) or (3.15) for the frequency $\tilde{\omega}$ in terms

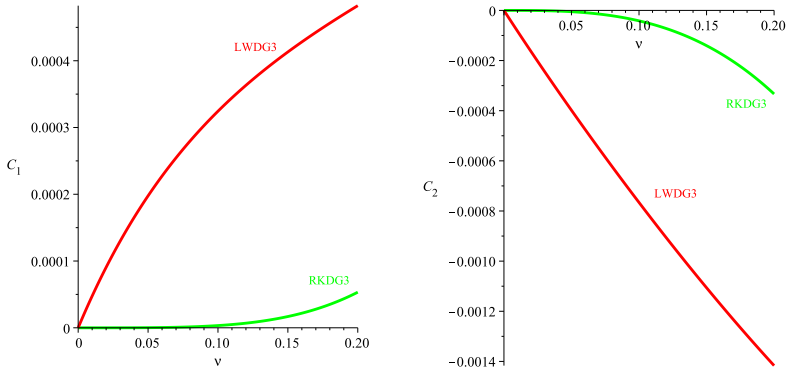


FIGURE 3.3. Left: The leading coefficient $C_1$ in the dispersion error $\Omega_r = K + C_1K^5 + O(K^7)$ for RKDG3 and LWDG3. Right: The leading coefficient $C_2$ in the dissipation error $\Omega_i = C_2K^4 + O(K^6)$ for RKDG3 and LWDG3.

of the wavenumber $k$. The advantage of this approach is the clearness of its physical meaning, since the wavenumber $k$ is usually given in the initial condition. However, when we use the $(N+1)^{st}$ order RKDG or LWDG method, in order to obtain the formulation of $e^{-i\tilde{\omega}\Delta t}$ in terms of $k$, a polynomial equation of degree $N+1$ needs to be solved, and this becomes more complicated for larger $N$. On the other hand, when solving the eigenvalue problem (3.15) for the LWDG method by computing the determinant of the coefficient matrix, if one solves the wavenumber in terms of the frequency, the eigenvalue problem will be much simpler. This is stated more rigorously in the next Theorem.

**Theorem 3.1.** *Suppose $h > 0, N \in \mathbb{N}$ and $\beta, \gamma \in [0,1]$. Consider the $(N+1)^{st}$ order LWDG method with the numerical flux defined in* (3.12)*, then the discrete dispersion relation is determined by the consistent solution of the eigenvalue problem* (3.15)*. Moreover, (i) For $N = 0$, the eigenvalue problem is a quadratic equation in terms of $\xi = e^{ikh}$ when $0 < \beta < 1$, and it is linear when $\beta = 0$ or $\beta = 1$. (ii) For $N \geq 1$, when $(\beta-1)^2 + (\gamma-1)^2 \neq 0$ and $\beta^2 + \gamma^2 \neq 0$, the eigenvalue problem is a quadratic equation in terms of $\xi = e^{ikh}$. When $\beta = \gamma = 1$ or $\beta = \gamma = 0$, the eigenvalue problem turns to a linear polynomial equation.*

*Proof.* The eigenvalue problem (3.15) has nontrivial solutions if and only if the determinant of the coefficient matrix $\mathcal{M}$ is equal to zero. The conclusion for $N = 0$ is straightforward, as all the involved matrices are scalar, we here only focus on the cases with $N \geq 1$. When $\beta$ and $\gamma$ are not equal to 0 or 1 at the same time, it is easy to show that matrices $E^+$ and $G^-$ are of rank 1. By the properties of determinant under row or column operations, the determinant of the matrix is of the form $\delta_1 + \delta_2 e^{ikh} + \delta_3 e^{-ikh}$, where $\delta_i, i = 1,2,3$ are constants. Therefore the solution of the eigenvalue problem

(3.15) is the root of $\delta_2\xi^2 + \delta_1\xi + \delta_3 = 0$ with $\xi = e^{ikh}$. When $\beta = \gamma = 1$, we have $E^+ = 0$ based on its definition in (3.13). In this case, the determinant can be reduced to $\delta_1 + \delta_3 e^{-ikh}$, thus the problem leads to a first order equation $\delta_1\xi + \delta_3 = 0$. Similarly, when $\beta = \gamma = 0$, we have $G^- = 0$ in (3.15). Following the same discussion, we can also obtain that the problem leads to a linear polynomial equation. □

Given the frequency $\omega$, $u(x,t) = e^{i(kx-\omega t)}$ is the exact solution for (3.1) with the wavenumber $k = \omega$. Assume the numerical solution of the LWDG methods is of the same form, namely, $u_h(x,t) = e^{i(\tilde{k}x-\omega t)}$. Following [2], we define the relative error $\rho_N = \frac{e^{ikh}-e^{i\tilde{k}h}}{e^{ikh}}$. Note that $\rho_N \approx i(k-\tilde{k})h$ with $K = kh \ll 1$, and it measures the difference between the exact and the discrete wavenumbers multiplied by the mesh parameter $h$ and therefore gives the dispersion error of the schemes. Theorem 3.1 implies that with the fixed-$\omega$ method, one can obtain the analytical formulation of the consistent eigenvalue for any $N$ and therefore the discrete dispersion relation for arbitrary order LWDG methods. This is a huge advantage over the standard approach. The fixed-$\omega$ approach was used in [2] to analyze the dispersion property for the semi-discrete DG methods of any order of accuracy.

For the commonly-used numerical flux given by (3.12) with $\beta = 1, \gamma = \frac{1}{2}$, we can easily compute the asymptotic formulation of the relative error $\rho_N$, and the results for $N = 0, 1, \ldots, 4$ are given as follows.

$$
\begin{aligned}
\rho_0 &= \left(\frac{1}{2} - \frac{\nu}{2}\right) K^2 + i\left(\frac{1}{3} - \frac{\nu}{2} + \frac{1}{6}\nu^2\right) K^3 + O(K^4) \\
\rho_1 &= i\left(\frac{1}{12}\nu + \frac{1}{6}\nu^2\right) K^3 + \left(\frac{1}{72} - \frac{1}{72}\nu - \frac{1}{6}\nu^2 - \frac{1}{8}\nu^3\right) K^4 + O(K^5) \\
\rho_2 &= -\frac{1}{120}\frac{\nu(5\nu^3 - 2\nu - 1)}{3\nu + 1} K^4 - \frac{i}{1800}\frac{(60\nu^5 + 15\nu^4 - 70\nu^3 - 8\nu - 9)\nu}{(3\nu+1)^2} K^5 + O(K^6) \\
\rho_3 &= -\frac{i}{5040}\frac{(35\nu^5 - 43\nu^3 + 20\nu + 3)\nu}{5\nu^2 + 1} K^5 \\
&+ \frac{1}{70560}\frac{(2975\nu^6 + 175\nu^5 - 4105\nu^4 - 470\nu^3 + 830\nu^2 + 316\nu + 24)\nu}{(5\nu^2+1)^2} K^6 + O(K^7) \\
\rho_4 &= \frac{1}{90720}\frac{(147\nu^7 - 455\nu^5 + 343\nu^3 - 20\nu - 3)\nu}{10\nu + 1} K^6 \\
&- \frac{i}{816480}\frac{\xi}{(1 + 20\nu + 100\nu^2)} K^7 + O(K^8)
\end{aligned}
$$

where $\xi = 9261\nu^{12} - 45570\nu^{10} - 1323\nu^9 + 56999\nu^8 + 855\nu^7 - 22842\nu^6 + 189\nu^5 + 2574\nu^4 + 165\nu^3 + 73\nu^2 + 15\nu$. For the linear advection equation (3.1), one can also consider the fully upwind numerical flux, namely (3.12) with $\beta = \gamma = 1$. When $N = 0$, $\rho_0$ has the same formulation as above. And

$\rho_N$, with $N = 1, \ldots, 4$, are given as follows.

$$\begin{aligned}
\rho_1 &= \frac{i}{12}\left(\nu - \nu^2\right) K^3 + \left(\frac{1}{72} - \frac{1}{18}\nu + \frac{1}{24}\nu^2\right) K^4 + O(K^5) \\
\rho_2 &= \frac{1}{120}\left(\nu - \nu^2\right) K^4 + i\left(\frac{1}{180}\nu^4 + \frac{1}{200}\nu - \frac{19}{1800}\nu^2\right) K^5 + O(K^6) \\
\rho_3 &= i\left(-\frac{1}{504}\nu^2 - \frac{1}{720}\nu^4 - \frac{1}{1680}\nu\right) K^5 \\
&+ \left(\frac{1}{2940}\nu - \frac{59}{70560}\nu^2 + \frac{1}{2016}\nu^4\right) K^6 + O(K^7) \\
\rho_4 &= \left(\frac{1}{9072}\nu^2 - \frac{1}{30240}\nu - \frac{1}{12960}\nu^4\right) K^6 \\
&+ i\left(\frac{11}{116640}\nu^2 - \frac{1}{54432}\nu - \frac{1}{3645}\nu^4 + \frac{1}{5040}\nu^6\right) K^7 + O(K^8)
\end{aligned}$$

Based on the formulations of $\rho_N$ for the LWDG methods using the numerical flux with $\beta = 1$, and $\gamma = \frac{1}{2}$ or 1, the following pattern can be observed,

$$\rho_N = \begin{cases} C_2 K^{N+3} + iC_1 K^{N+2} + O(K^{N+4}), & \text{if } N \text{ is odd,} \\ C_1 K^{N+2} + iC_2 K^{N+3} + O(K^{N+4}), & \text{if } N \text{ is even,} \end{cases} \tag{3.17}$$

where $C_1, C_2$ are two real constants dependent of the CFL number $\nu$ and $N$. These formulas show that the relative error $\rho_N$ is of order $N+2$ in $K \ll 1$ for the $(N+1)^{st}$ order LWDG methods. Here $C_1$ or $iC_1$ denotes the coefficient of the leading order term. The formulas can be used to further study the relative error. For instance, in Figure 3.4, $\ln(|C_1|)$ is plotted as a function of $\nu$ for the method with $\beta = 1$ and $\gamma = \frac{1}{2}$. One can conclude that when $N$ increases, not only $\rho_N$ will be of higher order accuracy, the magnitude of the leading coefficient $|C_1|$ will also decrease significantly. Since $\ln(|C_1|) \to -\infty$ as $\nu \to 0$, we only plot $\ln(|C_1|)$ for $\nu$ from $10^{-5}$ to 0.22.

*Remark* 3.2. (1) Though a similar result as in theorem 3.1 holds for the semi-discrete DG method in (3.2) (see [2]), it does not hold for fully discrete RKDG methods. It can be shown that the eigenvalue problem in the dispersion analysis for the RKDG3 method leads to a cubic polynomial equation in terms of $e^{ikh}$.

(2) $-\Re(\rho_N) \approx -\Im(\tilde{k}h)$ and $\Im(\rho_N) \approx \Re(kh - \tilde{k}h)$ measure the dissipation and dispersion errors of LWDG methods, respectively. This is consistent to the observation that for LWDG(N+1) with $N = 1, 2$, $-\Re(\rho_N)$ is of the same order of accuracy as $\Omega_i$, and $\Im(\rho_N)$ is of the same order of accuracy as $\Omega_r - K$.

One natural question is, can we design LWDG methods with a higher order relative error $\rho_N$ if the parameters $\beta$ and $\gamma$ take some special values in the numerical flux (3.12)? When $N = 0$, the numerical flux is given by

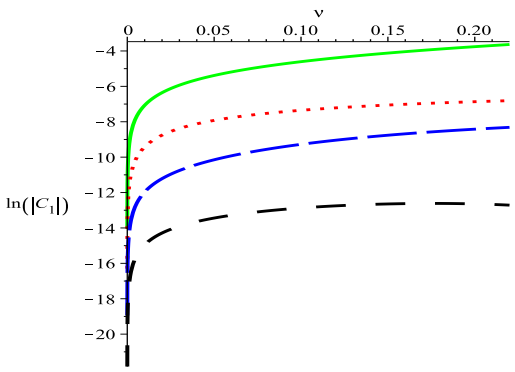


FIGURE 3.4. $\ln(|C_1|)$, with $C_1$ defined in (3.17), for the $(N+1)^{st}$ order LWDG method using the numerical flux (3.12) with $\beta = 1$ and $\gamma = \frac{1}{2}$, $N = 1, \ldots, 4$. The solid, dot, long-dash and space-dash lines represent the case when $N = 1, 2, 3, 4$ respectively.

$\hat{F} = \beta u^- + (1-\beta)u^+$, and the relative error is given as,

$$\rho_0 = (\beta - \frac{1+\nu}{2})K^2 + \frac{i}{6}(12\beta^2 - 6\nu\beta - 12\beta + \nu^2 + 3\nu + 2)K^3 + O(K^4).$$

One can see that for general value of $\beta$, there is $\rho_0 = O(K^2)$ and this is consistent to our previous observation. Yet when $\beta$ and the CFL number $\nu$ are properly related, namely, $\beta = \frac{1+\nu}{2}$, $\rho_0$ will be one order higher with $\rho_0 = O(K^3)$. In this case, the numerical flux becomes $\hat{F} = \frac{1+\nu}{2}u^- + \frac{1-\nu}{2}u^+$ which is upwind-biased. Numerical experiments with $\nu = 0.2, 0.4, 0.6, 0.8$ also indicates that the resulting method is stable. The success of the LWDG1 with $N = 0$ unfortunately can not be carried over to general $N$. For example, when $N = 1$ with $\hat{F} = \beta u^- + (1-\beta)u^+ - \frac{\Delta t}{2}(\gamma u_x^- + (1-\gamma)u_x^+)$, in order to improve the accuracy order of $\rho_1$ from $O(K^3)$ to $O(K^4)$, one needs $\beta = \frac{1}{2}$ and $\gamma = \frac{1}{2} + \frac{1}{6\nu}$. Note that $\nu$ appears in the denominator of $\gamma$ which grows unboundedly when $\nu$ approaches 0. Numerical tests show that the resulting method, though formally with higher order relative error $\rho_1$, is unstable.

## 4. The role of the spatial and the temporal discretizations

In section 3, we have derived the analytical formulations of the leading terms of the dispersion and dissipation errors, $\Omega_r - K$ and $\Omega_i$, of RKDG and LWDG methods, as well as the relative error $\rho_N$ for LWDG methods, as a function of the CFL number $\nu$. The analysis is carried out by assuming $\nu$ is a constant. In this section, we will further discuss these results when $\nu$ can depend on $K$ and therefore can be chosen to be "smaller", with the goal to understand the role of the spatial and the temporal discretization in the dispersion analysis for the fully discrete methods.

We start with RKDG methods. In section 3.1, we obtain for RKDG2 the dispersive error $\Omega_r - K = \frac{1}{6}\nu^2 K^3 + (\frac{1}{270} - \frac{1}{20}\nu^4)K^5 + O(K^7)$ which is third order accurate. Note that $\lim_{\nu\to 0} \frac{1}{6}\nu^2 = 0$ and $\lim_{\nu\to 0} \frac{1}{270} - \frac{1}{20}\nu^4 = \frac{1}{270}$. If $\nu$ is taken to be "smaller", in particular with $\nu = O(K^r)$ and $r \geq 1$, then $\Omega_r - K = O(K^5)$ and it is two order more accurate. On the other hand, smaller $\nu$ will not change the overall fourth order accuracy of the dissipative error $\Omega_i = (-\frac{1}{72} + \frac{1}{8}\nu^3)K^4 + O(K^6) = O(K^4)$. Since the properties of the fully discrete schemes with sufficiently small CFL numbers are determined only by spatial discretizations, one can conclude that the second order DG spatial discretization contributes to RKDG2 with $\Omega_r - K = O(K^5)$ and $\Omega_i = O(K^4)$, yet the second order Runge-Kutta time discretization reduces the order of the dispersive error by two while keeping the dissipative error unchanged. Similarly, for RKDG3, from the dispersion analysis given in (3.11), and with the sufficiently small CFL number, namely $\nu = O(K^r)$ and $r \geq \frac{2}{3}$, the dispersive error becomes $\Omega_r - K = O(K^7)$ and the dissipative error is $\Omega_i = O(K^6)$, and these can be attributed to the third order DG spatial discretization, while the third order Runge-Kutta time discretization reduces the order of both dispersive and dissipative errors by two, rendering $\Omega_r - K = O(K^5)$ and $\Omega_i = O(K^4)$.

Next we consider LWDG methods. For LWDG2, the dispersion and dissipation errors are given as

$$\begin{cases} \Omega_r = K + (\frac{1}{12}\nu + \frac{1}{6}\nu^2)K^3 + (\frac{1}{270} + \frac{5}{432}\nu - \frac{11}{144}\nu^2 - \frac{1}{8}\nu^3 - \frac{1}{20}\nu^4)K^5 + O(K^7), \\ \Omega_i = (-\frac{1}{72} + \frac{1}{72}\nu + \frac{1}{6}\nu^2 + \frac{1}{8}\nu^3)K^4 + (\frac{1}{648} + \frac{17}{2592}\nu - \frac{29}{864}\nu^2 - \frac{7}{96}\nu^3 - \frac{1}{20}\nu^4)K^6 + O(K^8). \end{cases}$$

With $\nu = O(K^r)$ and $r \geq 2$, we have $\Omega_r - K = O(K^5)$ and $\Omega_i = O(K^4)$, and they are determined by the spatial discretization in LWDG2, while the time discretization in LWDG2 is responsible for $\Omega_r - K = O(K^3)$ and $\Omega_i = O(K^4)$. For LWDG3, there is

$$\begin{cases} \Omega_r = & K - \frac{1}{1800}\frac{(60\nu^5+15\nu^4-70\nu^3-8\nu-9)\nu}{(1+3\nu)^2}K^5 + \frac{\xi}{3780000(1+3\nu^4)}K^7 + O(K^8), \\ \Omega_i = & \frac{1}{120}\frac{(5\nu^3-2\nu-1)\nu}{1+3\nu}K^4 - \\ & \frac{1}{36000}\frac{1500\nu^8+750\nu^7-2150\nu^6-3075\nu^5+830\nu^4+1950\nu^3+439\nu^2-33\nu+5}{(1+3\nu)^3}K^6 + O(K^8), \end{cases}$$

with $\xi = 45000\nu^{10} + 33750\nu^9 - 148500\nu^8 + 27375\nu^7 - 94100\nu^6 - 142275\nu^5 + 97415\nu^4 + 129000\nu^3 + 24327\nu^2 - 2994\nu + 90$. Then with $\nu = O(K^r)$ and $r \geq 2$, the dispersion and dissipation errors of LWDG3 are $\Omega_r - K = O(K^7)$ and $\Omega_i = O(K^6)$, and they are attributed to the spatial discretization of LWDG3, while its temporal discretization is responsible for the two order lower dispersive error $\Omega_r - K = O(K^5)$ and the dissipative error $\Omega_i = O(K^4)$ of the fully discrete LWDG3. Compared with RKDG(N+1), $N = 1$ or 2, in order to extract the contribution of the spatial discretization, one needs to use relatively smaller $\nu$ and therefore smaller time-step $\Delta t$ in LWDG(N+1).

Based on the analysis given so far, one can see that with sufficiently small CFL numbers, both RKDG and LWDG methods have a $(2N+3)^{rd}$ order dispersive error $\Omega_r - K$, and a $(2N+2)^{nd}$ order dissipative error

$\Omega_i$ where $N = 1, 2$. Since these orders of accuracy are higher than the expected $(N+1)^{st}$ order of accuracy of the methods in the $L^2$ norm, the spatial discretizations of both RKDG and LWDG methods lead to *super-convergence* in dispersion and dissipation errors. When the wavenumber $k$ is given, by taking into account the factor $h$ in $\Omega_r$ and $\Omega_i$, we also say that the dispersive error $\omega_r - k$ due to the spatial discretization is $(N+1)^{st}$ order more accurate and the dissipative error $\omega_i$ is $N^{th}$ order more accurate than the $L^2$ errors of the RKDG or LWDG numerical solutions. On the other hand, the temporal discretization reduces the super-convergence in the dispersive error when $N = 2$, while completely eliminating the super-convergence in the dispersive error when $N = 1$ and in the dissipative error when $N = 2$.

Finally, we turn our discussion to the relative error $\rho_N$ obtained for the LWDG methods in section 3.4. With the similar analysis as for $\Omega_r - K$ and $\Omega_i$, based on $\rho_N$, $N = 0, \ldots, 5$ of the LWDG methods using the numerical flux (3.12) with $\beta = 1$ and $\gamma = \frac{1}{2}$, and with the CFL number $\nu = O(K^r)$ and $r \geq N + 2$ for $K \ll 1$, we obtain

(4.1)
$$\rho_N = \frac{1}{2}\left(\frac{N!}{(2N+1)!}\right)^2 K^{2N+2} + i\left(\frac{N!}{(2N+1)!}\right)^2 \frac{N+1}{(2N+1)(2N+3)} K^{2N+3} + O(K^{2N+4}).$$

We conjecture that (4.1) also holds for general $N$. One can see that $\rho_N$ for LWDG methods is of $(2N+2)^{nd}$ order accuracy if the influence of time discretizations can be neglected, and this is a super-convergent property, similar as previously discussed for $\Omega_r - K$ and $\Omega_i$. In [2], the asymptotic formulations of the relative error $\rho_N$ was mathematical proved for the semi-discrete upwind DG method in (3.2) with any $N$. In this case $\rho_N$ is completely determined by the spatial DG discretizations. Although LWDG methods do not have a semi-discrete version when $\Delta t \to 0$, one can still compare $\rho_N$ in (4.1) and that in [2]. Indeed, the formula of $\rho_N$ in (4.1) is identical to that of the semi-discrete upwind DG method in (3.2). Hence the spatial discretization of LWDG methods contributes to $\rho_N$ in a similar way as that of the semi-discrete DG methods. The results in section 3.4 show that $\rho_N$ is of order $(N+2)$ with $\nu = O(1)$, indicating that the time discretization eliminates the super-convergence in $\rho_N$. (Recall that $\rho_N \approx i(k - \tilde{k})h$.) Although the formulas of $\rho_N$ for LWDG methods with $\beta = 1, \gamma = \frac{1}{2}$ and $\beta = \gamma = 1$ are quite different, we can show that with the CFL number $\nu = O(K^r)$ and $r \geq N + 2$, (4.1) is also satisfied for LWDG methods with $\beta = \gamma = 1$. Therefore the spatial discretization of LWDG methods with those two types of numerical fluxes has similar effect on $\rho_N$.

## 5. Numerical experiments

In this section, we will present a set of numerical experiments, which will verify some of the theoretical findings in sections 3 and 4 and demonstrate the dispersion and dissipation behavior of the RKDG and LWDG methods

with $N = 1, 2$. A simple cosine wave will be considered in section 5.1, followed by a non-smooth square wave in section 5.2.

5.1. **Cosine wave.** We start with the linear advection equation in (3.1) with a smooth initial condition $u(x, 0) = \cos(4x)$ and a periodic boundary condition. This simple cosine wave will be simulated by RKDG methods and LWDG methods up to the final time $T$ on a uniform mesh with $m$ elements. For LWDG methods, the numerical flux is given by (3.12) with $\beta = 1, \gamma = \frac{1}{2}$.

We first take the CFL number to be constant, with $\nu = \frac{1}{3}$ for RKDG2, $\nu = 0.2$ for LWDG2, $\nu = 0.2$ for RKDG3, and $\nu = 0.1$ for LWDG3. In Figure 5.1, we plot the numerical solutions of RKDG2 and LWDG2 methods with $m = 100$ and $T = 400\pi$. One can see that the RKDG2 is more dissipative. The solutions by RKDG3 and LWDG3 methods are given in Figure 5.2 on the same mesh at $T = 400\pi$. Apparently, these two third order methods perform much better than the second order ones. In fact, one would need to zoom in the plot (see the one on the right in Figure 5.2) in order to see the difference among the two numerical solutions and the exact solution. This zoomed-in plot also shows that the LWDG3 method is more dissipative than the RKDG3 method. These qualitative observations are consistent to our theoretical analysis. What one cannot directly extract from these two figures is the phase error in the numerical solutions.

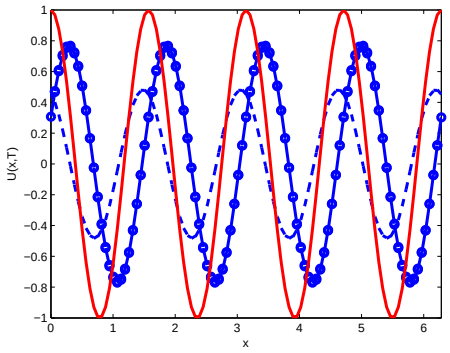


FIGURE 5.1. The exact solution (solid line), and the numerical solutions of RKDG2 (dashed line) and LWDG2 (dash-circle line) methods, with the initial condition $u(x, 0) = \cos(4x)$ and the final time $T = 400\pi$ on a uniform mesh with $m = 100$.

Next, we will examine the dissipation and dispersion errors quantitatively and verify the analytical results in section 3. More specifically, we want to estimate the orders $N_1$ and $N_2$ in the dispersion error $\Omega_r - K = O(K^{N_1})$ and the dissipation error $\Omega_i = O(K^{N_2})$. With the initial condition $u(x, 0) = e^{ikx}$ and the numerical solution $u_h$ (resp. $u_H$) computed from a uniform mesh

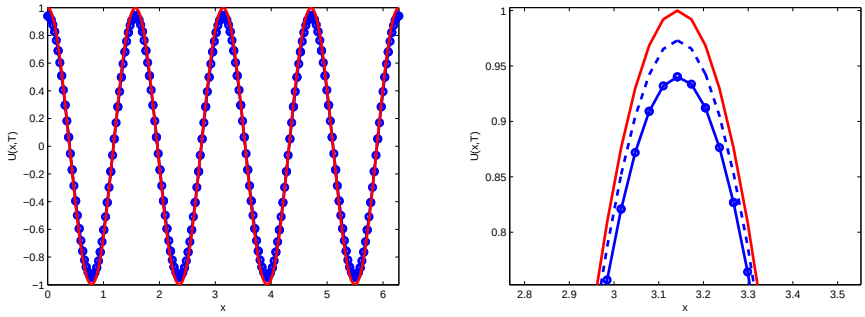


FIGURE 5.2. The exact solution (solid line), and the numerical solutions of RKDG3 (dashed line) and LWDG3 (dash-circle line) methods, with the initial condition $u(x,0) = \cos(4x)$ and the final time $T = 400\pi$ on a uniform mesh with $m = 100$. The zoomed-in plot is given on the right.

with the meshsize $h$ (resp. $H$), $N_2$ can be obtained based on (3.10) as follows,

$$N_2 = \frac{\ln\left(\ln|u_h|/\ln|u_H|\right)}{\ln(h/H)} + 1.$$

Since we are using $\Re(u(x,0))$ as the initial condition in the simulation, $N_2$ is indeed computed as

$$N_2 = \frac{\ln\left(\ln(\max|u_h|)/\ln(\max|u_H|)\right)}{\ln(h/H)} + 1.$$

To estimate $N_1$, one would need to manually track the phase shift between the numerical and the exact solutions at time $T$. Let $d_h$ (resp. $d_H$) denote the phase distance between the exact and the numerical solutions which are originally at $x = 0$. Then $d_h = \frac{\Omega_{r,h} - kh}{h} T$, and

$$N_1 = \frac{\ln\left(\ln d_h/\ln d_H\right)}{\ln(h/H)} + 1. \tag{5.1}$$

Note that we are not taking absolute values of $d_h$ and $d_H$ in (5.1) due to that both fully discrete DG methods exhibit phase lead. This has been implied by the analysis in Section 3.3 and can also be seen from Table 5.1 and Table 5.3. Since we determine $d_h$ by counting the number of involved mesh elements, $d_h$ is accurate only up to $\pm h$.

In Table 5.1, we report the dispersion and dissipation errors and orders of RKDG2 and LWDG2 based on the numerical solution at time $T = 400\pi$. The results confirm the third order dissipation error and the fourth order dispersion error predicted by our analysis in sections 3.1.1 and 3.2.1. We can also see that RKDG2 is less dispersive (with smaller $d_h$) but more dissipative (with larger $|\ln(\max|u_h|)|$. When $N = 2$, it is difficult to track the phase distance $d_h$, therefore in Table 5.2 we only report the dissipation errors and

orders of RKDG3 and LWDG3, which again verify the theoretical results that the dissipation errors are fourth order for both methods, with LWDG3 being more dissipative.

TABLE 5.1. Dispersion and dissipation errors and orders of RKDG2 with $\nu = 1/3$ and LWDG2 with $\nu = 0.2$ at $T = 400\pi$. The initial condition is $u(x, 0) = \cos(4x)$.

| | RKDG2 | | | | LWDG2 | | | |
|---|---|---|---|---|---|---|---|---|
| $m$ | $d_h$ | $\ln(\max\|u_h\|)$ | $N_1$ | $N_2$ | $d_h$ | $\ln(\max\|u_h\|)$ | $N_1$ | $N_2$ |
| 50 | $\frac{49}{25}\pi$ | -5.76E-0 | - | - | $\frac{12}{5}\pi$ | -2.03E-0 | - | - |
| 100 | $\frac{12}{25}\pi$ | -7.25E-1 | 3.03 | 3.99 | $\frac{3}{5}\pi$ | -2.61E-1 | 3.00 | 3.96 |
| 200 | $\frac{3}{25}\pi$ | -9.02E-2 | 3.00 | 4.01 | $\frac{3}{20}\pi$ | -3.21E-2 | 3.00 | 4.02 |
| 400 | $\frac{3}{100}\pi$ | -1.09E-2 | 3.00 | 4.05 | $\frac{7}{200}\pi$ | -3.91E-3 | 3.10 | 4.04 |
| Exact | 0 | 0 | 3 | 4 | 0 | 0 | 3 | 4 |

TABLE 5.2. Dissipation errors and orders of RKDG3 with $\nu = 0.2$ and LWDG3 with $\nu = 0.1$ at $T = 400\pi$. The initial condition is $u(x, 0) = \cos(4x)$.

| | RKDG3 | | LWDG3 | |
|---|---|---|---|---|
| $m$ | $\ln(\max\|\tilde{u}\|)$ | $N_2$ | $\ln(\max\|\tilde{u}\|)$ | $N_2$ |
| 50 | -2.34E-1 | - | -5.05E-1 | - |
| 100 | -2.72E-2 | 4.10 | -6.17E-2 | 4.04 |
| 200 | -3.34E-3 | 4.03 | -7.66E-3 | 4.01 |
| 400 | -4.16E-4 | 4.01 | -9.56E-4 | 4.00 |
| Exact | 0 | 4 | 0 | 4 |

The results in Tables 5.1-5.2 are computed when the CFL number $\nu$ is taken to be constant during the mesh refinement. Now we want to investigate the performance of the methods when $\nu = O(K^r)$, that is, $\nu$ depends on the meshsize, with $r$ properly chosen according to section 3.4. The objective is to numerically verify the super-convergence in the dissipation and dispersion errors when the contribution of the time discretizations can be negligible.

Due to the difficulty in measuring the phase shift $d_h$ for highly accurate methods, we carry out the simulations to the final time $T = 800\pi$ on meshes with $m = 130, 150, 170, 190$. In Table 5.3, the dissipation and dispersion errors and orders are presented for RKDG2 with $\nu = K$ and for LWDG2 with $\nu = K^2$. Note that the order of the dissipation errors is 4 as predicted in section 3.4, while the order of dispersion errors oscillates around the theoretical value 5. The latter is due to the $\pm h$ measuring error in $d_h$. Table 5.4 reports the dissipation errors and orders of RKDG3 with $\nu = K$ and of

LWDG3 with $\nu = K^2$. They confirms the super-convergence in dissipation errors, which are of sixth order accurate and are only due to the spatial discretization.

TABLE 5.3. Dispersion and dissipation errors and orders of RKDG2 with $\nu = K$ and LWDG2 with $\nu = K^2$ at $T = 800\pi$. The initial condition is $u(x, 0) = \cos(4x)$.

| | RKDG2 | | | | LWDG2 | | | |
|---|---|---|---|---|---|---|---|---|
| $m$ | $d_h$ | $\ln(\max\|u_h\|)$ | $N_1$ | $N_2$ | $d_h$ | $\ln(\max\|u_h\|)$ | $N_1$ | $N_2$ |
| 130 | $\frac{12}{65}\pi$ | -9.34E-1 | - | - | $\frac{7}{65}\pi$ | -9.43E-1 | - | - |
| 150 | $\frac{8}{75}\pi$ | -6.23E-1 | 4.83 | 3.83 | $\frac{4}{75}\pi$ | -6.25E-1 | 5.91 | 3.87 |
| 170 | $\frac{1}{17}\pi$ | -4.34E-1 | 5.76 | 3.89 | $\frac{3}{85}\pi$ | -4.34E-1 | 4.30 | 3.92 |
| 190 | $\frac{4}{95}\pi$ | -3.13E-1 | 4.01 | 3.93 | $\frac{2}{95}\pi$ | -3.13E-1 | 5.65 | 3.94 |
| Exact | 0 | 0 | 5 | 4 | 0 | 0 | 5 | 4 |

TABLE 5.4. Dissipation errors and orders of RKDG3 with $\nu = K$ and LWDG3 with $\nu = K^2$ at $T = 800\pi$. The initial condition is $u(x, 0) = \cos(4x)$.

| | RKDG3 | | LWDG3 | |
|---|---|---|---|---|
| $m$ | $\ln(\max\|\tilde{u}\|)$ | $N_2$ | $\ln(\max\|\tilde{u}\|)$ | $N_2$ |
| 130 | -2.24E-2 | - | -2.21E-2 | - |
| 150 | -9.59E-3 | 6.92 | -1.09E-2 | 5.94 |
| 170 | -4.61E-3 | 6.85 | -5.87E-3 | 5.95 |
| 190 | -2.31E-3 | 7.20 | -3.38E-3 | 5.96 |
| Exact | 0 | 6 | 0 | 6 |

5.2. **Square wave.** In this subsection, we consider the advection equation (3.1) with the following initial condition,

$$u(x,0) = \begin{cases} 1, x \in [\frac{\pi}{2}, \frac{3\pi}{2}], \\ 0, x \in [0, \frac{\pi}{2}) \cup (\frac{3\pi}{2}, 2\pi]. \end{cases} \tag{5.2}$$

which can be decomposed into infinite cosine waves

$$u(x,0) = \frac{1}{2} + \frac{2}{\pi}\sum_{k=0}^{\infty}(-1)^{k+1}\frac{\cos[(2k+1)x]}{2k+1}. \tag{5.3}$$

The exact solution is a square wave.

In Figure 5.3, the numerical solutions of RKDG2 and LWDG2 are plotted against the exact solution at $T = 2\pi$. Note that both numerical solutions display oscillations, which are due to dispersion errors of the methods, especially the different dispersion errors associated with each individual cosine mode. At this time, one can not tell which method has larger dispersion

error. On the other hand, the magnitude of the oscillation in RKDG2 solutions is relatively smaller, this indicates that RKDG2 is more dissipative, just as predicted by the theoretical result in section 3 for a single wave mode.

The analysis in section 3 implies that higher order methods have better dissipation and dispersion behavior and therefore more accurate results, this can be demonstrated by Figure 5.4 which includes the solutions of RKDG3 and LWDG3. Note that these solutions have much smaller oscillations than the solutions by second order schemes, and the shape is also very close to the square wave. In order to compare the dissipation behaviors of RKDG3 and LWDG3, we continue the simulation and plot the solutions after $2.5 \times 10^4$ time periods in Figure 5.5. One can easily see that the LWDG3 is more dissipative and this agrees with our theoretical result in section 3.3. For the simulation in this subsection, we take the CFL number $\nu = \frac{1}{3}$ for RKDG2, $\nu = 0.2$ for LWDG2, $\nu = 0.2$ for RKDG3, and $\nu = 0.1$ for LWDG3.

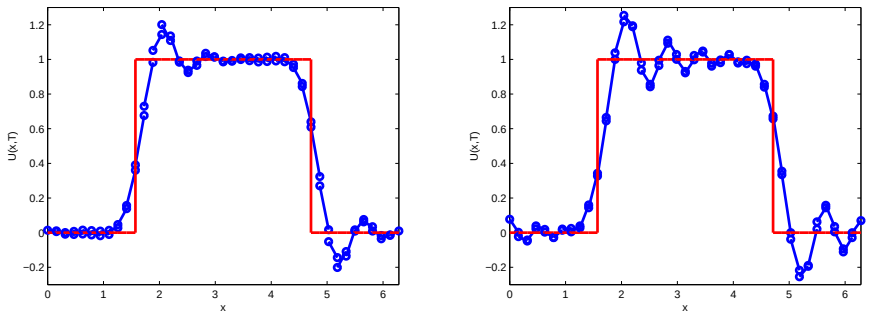


FIGURE 5.3. Solutions by RKDG2 (left) and LWDG2 (right), with a square wave initial condition (5.2) and the final time $T = 2\pi$ on a uniform mesh with $m = 40$. The solid line and dash-circle line represent the exact solution and the numerical solution, respectively.

## 6. Concluding remarks

In this paper, the dispersion and dissipation errors are analyzed for discontinuous Galerkin methods. We focus on fully discrete discontinuous Galerkin methods and their analytical discrete dispersion relation as a function of the CFL number $\nu$ in the limit of $K = kh \to 0$. With the results, a quantitative comparison is made between Runge-Kutta discontinuous Galerkin methods (RKDG) and Lax-Wendroff discontinuous Galerkin methods (LWDG). In particular, for RKDG2 and LWDG2, the dominating error comes from dispersion, and RKDG2 has smaller dispersion error but larger dissipation error than LWDG2. However, RKDG3 has better dispersion and dissipation behavior than LWDG3. An alternative dispersion analysis, by assuming the wave frequency is given, proves to be advantageous for the one-step LWDG

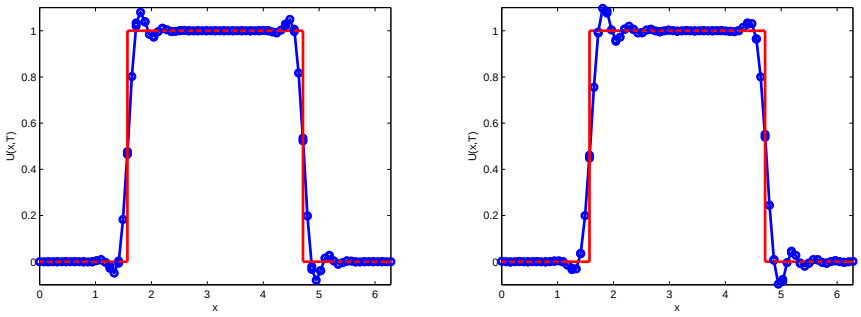


FIGURE 5.4. Solutions by RKDG3 (left) and LWDG3 (right), with a square wave initial condition (5.2) and the final time $T = 2\pi$ on a uniform mesh with $m = 40$. The solid line and dash-circle line represent the exact solution and the numerical solution, respectively.

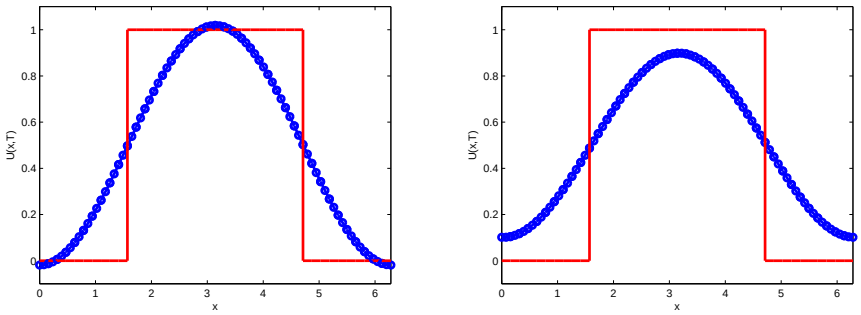


FIGURE 5.5. Solutions by RKDG3 (left) and LWDG3 (right), with a square wave initial condition (5.2) and the final time $T = 5 \times 10^4\pi$ on a uniform mesh with $m = 40$. The solid line and dash-circle line represent the exact solution and the numerical solution, respectively.

methods of arbitrary order of accuracy. This approach avoids solving an eigenvalue problem of a growing size when the accuracy order of the method increases.

By considering the dispersion and dissipation errors with sufficiently small CFL numbers, we also find that the DG spatial discretizations contributes to super-convergence in dissipation and dispersion errors, while the Runge-Kutta or Lax-Wendroff time discretizations with matching accuracy will reduce or eliminate such super-convergence when the CFL number is taken to be order one as in common practice. We believe this difference is due to that DG spatial discretizations are of finite element type, while the temporal discretizations in both RKDG and LWDG methods are of finite difference

type. To avoid or to reduce the loss of the super-convergence property, one can use $\nu = O(K^r)$ with some $r > 0$. That is, the CFL number depends on the meshsize and the characteristic wavenumber. Alternatively, when $\nu$ is chosen to be $O(1)$, one can employ higher order Runge-Kutta time discretizations for RKDG methods. In both cases, additional computational cost is needed. For LWDG methods with $\nu = O(1)$, completely different strategies need to be explored in order to preserve the super-convergence in dissipation and dispersion errors. This is currently under investigation.

The analysis in this paper is for the simple one dimensional scalar advection equation. One can also conduct similar dispersion analysis for higher dimensional or systems of wave equations. Though the actual analysis often depends on the choice of the discrete spaces and mesh elements, in some cases, it can be essentially one dimensional and scalar. For example, the dispersion analysis of RKDG methods for higher dimensional scalar advection equation can be reduced to the study of several one dimensional scalar advection equations, when the Cartesian mesh is used together with discrete spaces of tensor structure.

## References


[1] N. N. Abboud and P. M. Pinsky, Finite-element dispersion analysis for the 3-dimensional 2nd-order scalar wave-equation, International Journal for Numerical Methods in Engineering, 35 (1992), pp. 1183-1218.

[2] M. Ainsworth, Dispersive and dissipative behavior of high order discontinuous Galerkin finite element methods, Journal of Computational Physics, 198 (2004), pp.106-130.

[3] M. Ainsworth, Discrete dispersion relation for hp-version finite element approximation at high wave number, SIAM Journal on Numerical Analysis, 42 (2004), pp. 553-575.

[4] M. Ainsworth, P. Monk and W. Muniz, Dispersive and dissipative properties of discontinuous Galerkin finite element methods for the second-order wave equation, Journal of Scientific Computing, 27 (2006), pp. 5-60.

[5] M. Ainsworth and H. A. Wajid, Dispersive and dissipative behavior of the spectral element method, SIAM Journal on Numerical Analysis, 47 (2009), pp. 3910-3937.

[6] M. Ainsworth and H. A. Wajid, Explicit discrete dispersion relations for the acoustic wave equation in d-dimensions using finite element, spectral element and optimally blended schemes, Computer Methods in Mechanics, 1 (2010), pp. 3-17.

[7] G. Chavent and G. Salzano, A finite element method for the 1d water flooding problem with gravity, Journal of Computational Physics, 45 (1982), pp.307-344.

[8] B. Cockburn and C. W. Shu, The Runge-Kutta local projection $P^1$-discontinuous Galerkin method for scalar conservation laws, Mathematical Modelling and Numerical Analysis, 25 (1991), pp.337-361.

[9] B. Cockburn and C. W. Shu, TVB Runge-Kutta local projection discontinuous Galerkin finite element method for conservation laws II: general framework, Mathematics of Computation, 52 (1989), pp.411-435.

[10] J.S. Hesthaven and T. Warburton, Nodal high order methods on unstructured grids: I. time-domain solution of Maxwell's equations, Journal of Computational Physics, 181 (2002), pp. 186-221.

[11] F. Hu and H. Atkins, Eigensolution analysis of the discontinuous Galerkin method with non-uniform grids, part I: one space dimension, Journal of Computational Physics, 182 (2002), pp. 516-545.
[12] F. Hu, M. Hussaini and P. Rasetarinera, An analysis of the discontinuous Galerkin method for wave propagation problems, Journal of Computational Physics, 151 (1999), pp.921-946.
[13] F. Ihlenburg and I. Babuška, Dispersion analysis and error estimation of Galerkin finite element methods for the Helmholtz equation, International Journal for Numerical Methods in Engineering, 38 (1995), pp.3745-3774.
[14] C. Johnson and J. Pitkäranta, An analysis of the discontinuous Galerkin method for a scalar hyperbolic equation, Mathematics of Computation, 46 (1986), pp.1-26.
[15] P. Lesaint and P. A. Raviart, On a finite element method for solving the neutron transport equation, Mathematical Aspects of Finite Elements in Partial Differential Equations, Academic Press, New York, 1974, pp. 89-123.
[16] T. Peterson, A note on the convergence of the discontinuous Galerkin method for a scalar hyperbolic equation, SIAM Journal on Numerical Analysis, 28 (1991), pp. 133-140.
[17] J. Qiu, A numerical comparison of the Lax-Wendroff discontinuous Galerkin method based on different numerical fluxes, Journal of Scientific Computing, 30 (2007), pp. 345-367.
[18] J. Qiu, D. Michael and C.-W. Shu, The discontinuous Galerkin method with Lax-Wendroff type time discretizations, Computer Methods in Applied Mechanics and Engineering, 194 (2005), pp.4528-4543.
[19] W. H. Reed and T. R. Hill, Triangular mesh methods for the neutron transport equation, Technical Report LA-UR-73-479 (1973), Los Alamos Scientific Laboratory.
[20] G. R. Richter, An optimal-order error estimate for the discontinuous Galerkin method, Mathematics of Computation, 50 (1988), pp.75-88.
[21] D. Sármány, M. A. Botchev and J.J.W. van der Vegt, Dispersion and dissipation error in high-order Runge-Kutta discontinuous Galerkin discretizations of the Maxwell equations, Journal of Scientific Computing, 33 (2007), pp.47-74.
[22] S. Sherwin, Dispersive analysis of the continuous and discontinuous Galerkin formulations, lecture notes.
[23] D. Stanescu, D. A. Kopriva and M. Y. Hussaini, Dispersive analysis for discontinuous spectral element methods, Journal of Scientific Computing, 15 (2000), pp.149-171.
[24] Q. Zhang and C.-W. Shu, Error estimates to smooth solution of Runge-Kutta discontinuous Galerkin methods for scalar conservation laws, SIAM Journal on Numerical Analysis, 42 (2004), pp. 641-666.
[25] Q. Zhang and C.-W. Shu, Error estimates to smooth solution of Runge-Kutta discontinuous Galerkin methods for symmetrizable conservation laws, SIAM Journal on Numerical Analysis, 44 (2006), pp. 1702-1720.
[26] Q. Zhang and C.-W. Shu, Stability analysis and a priori error estimates to the third order explicit Runge-Kutta discontinuous Galerkin method for scalar conservation laws, SIAM Journal on Numerical Analysis, 48(2) (2010), pp. 772-795.
[27] X. Zhong and C.-W. Shu, Numerical resolution of discontinuous Galerkin methods for time dependent wave equations, Computer Methods in Applied Mechanics and Engineering, 200 (2011), pp. 2814-2827.

Department of Mathematical Sciences, Rensselaer Polytechnic Institute, 110 8th Street, Troy, New York, 12180, USA
*E-mail address*: yangh8@rpi.edu

Department of Mathematical Sciences, Rensselaer Polytechnic Institute, 110 8th Street, Troy, New York, 12180, USA
*E-mail address*: lif@rpi.edu

School of Mathematical Science, Xiamen University, Xiamen, Fujian, 361005, P.R. China
*E-mail address*: jxqiu@xmu.edu.cn